

Two nonmagnetic impurities in the DSC and DDW state of the cuprate superconductors as a probe for the pseudogap

Brian Møller Andersen

Ørsted Laboratory, Niels Bohr Institute, Universitetsparken 5, DK-2100 Copenhagen Ø, Denmark
(October 30, 2018)

The quantum interference between two nonmagnetic impurities is studied numerically in both the d-wave superconducting (DSC) and the d-density wave (DDW) state. In all calculations we include the tunnelling through excited states from the CuO₂ planes to the BiO layer probed by the STM tip. Compared to the single impurity case, a systematic study of the modulations of the two-impurity local density of states can distinguish between the DSC or DDW states. This is important if the origin of the pseudogap phase is caused by preformed pairs or DDW order. Furthermore, in the DSC state the study of the LDOS around two nonmagnetic impurities provide further tests for the potential scattering model versus more strongly correlated models.

74.72.-h, 72.10.Fk, 71.55.-i

I. INTRODUCTION

The study of magnetic and nonmagnetic impurities in the CuO₂ planes of the High-T_c superconductors is far from settled. Experimentally, the local density of states (LDOS) measured by scanning tunneling microscopy (STM) in Bi₂Sr₂CaCu₂O_{8+δ} (BSCCO) around a nonmagnetic impurity such as Zn displays a sharp peak close to the Fermi level on the impurity site and a second maximum on the next-nearest neighbor sites^{1,2}. Theoretically, the question remains whether a traditional potential scattering formalism^{3,4} or more strongly correlated models⁵ are needed to describe the impurity effects. Though still a subject of controversy, it was recently shown that at least for *weak* impurities a potential scattering scenario qualitatively agrees with the measured results for optimally doped BSCCO^{6–10}. Furthermore, it was shown by Martin *et al.*¹¹ that both the energetics and the spatial dependence of the resonance state around a strong potential scatterer (e.g. Zn) can be accounted for by including the tunnelling (the filter) through excited states from the CuO₂ planes to the top BiO layer probed by the STM tip¹². There is also evidence from nuclear magnetic resonance (NMR) measurements that magnetic moments are induced around nonmagnetic impurities¹³. In this paper we assume, however, that the large potential scattering off the impurity site *itself* is dominating the final LDOS.

Recently the experimental ability to manipulate the positions of surface impurities has increased the interest in quantum interference phenomena between multiple impurities. This includes the physics of quantum mirages¹⁴ and various multiple impurity effects in superconductors^{15–18}. For example, it was shown in Ref. 17 that impurity interference can be utilized as a sensitive probe for the gap symmetry of exotic superconductors. Motivated by the experimental progress we compare the expected LDOS around one and two strong nonmagnetic impurities in either the d-wave superconducting

(DSC) or the d-density wave (DDW) state. Though still controversial we include the filter effect in all the calculations presented below. As has become clear only recently^{15–17}, we stress that the probed impurities need be well separated (10-50 lattice constants) from other possible defects.

The DDW state was recently proposed as a model for the pseudo-gap state of the cuprates¹⁹. Any difference in the impurity modified LDOS between the DSC and DDW states may reveal the hidden DDW order and distinguish between the scenario of preformed pairs versus static staggered orbital currents as the origin for the pseudo-gap state^{20–22}. Recently, there has been several other proposals to probe the DDW order in the cuprates^{23,24}.

II. MODEL

In this section we briefly discuss the models for the DSC and DDW states and how to calculate the LDOS around several impurities. The BCS Greens function $\hat{G}^0(\mathbf{k}, i\omega_n)$ for the unperturbed d-wave superconductor is given by

$$\hat{G}^0(\mathbf{k}, i\omega_n) = [i\omega_n \hat{\tau}_0 - \xi(\mathbf{k}) \hat{\tau}_3 - \Delta(\mathbf{k}) \hat{\tau}_1]^{-1}, \quad (1)$$

where $\hat{\tau}_\nu$ denotes the Pauli matrices in Nambu space, $\hat{\tau}_0$ being the 2×2 identity matrix, $\xi(\mathbf{k})$ the quasi-particle dispersion, and ω_n is a Matsubara frequency. For a system with d_{x²-y²}-wave pairing symmetry, $\Delta(\mathbf{k}) = \frac{\Delta_0}{2} (\cos(k_x) - \cos(k_y))$. In the DDW state the mean-field Hamiltonian is given by¹⁹

$$H = \sum_{\mathbf{k}\sigma} \xi(\mathbf{k}) c_{\mathbf{k}\sigma}^\dagger c_{\mathbf{k}\sigma} + i \sum_{\mathbf{k}\sigma} D(\mathbf{k}) c_{\mathbf{k}\sigma}^\dagger c_{\mathbf{k}+\mathbf{Q}\sigma} \quad (2)$$

where $c_{\mathbf{k}\sigma}^\dagger$ creates an electron with momentum \mathbf{k} and spin σ , $\mathbf{Q} = (\pi, \pi)$ and $D(\mathbf{k}) = \frac{D_0}{2} (\cos(k_x) - \cos(k_y))$. Be-

low, $\Delta_0 = D_0 = 50\text{meV}$ and the lattice constant is set to unity. The large value of the gap corresponds roughly to the experimentally measured maximum gap in the underdoped regime of BSCCO.

The Greens function for the clean DDW state is given by

$$\hat{G}^0(\mathbf{k}, i\omega_n) = \frac{\begin{pmatrix} i\omega_n - \xi(\mathbf{k} + \mathbf{Q}) & -iD(\mathbf{k}) \\ iD(\mathbf{k}) & i\omega_n - \xi(\mathbf{k}) \end{pmatrix}}{(i\omega_n - \xi(\mathbf{k}))(i\omega_n - \xi(\mathbf{k} + \mathbf{Q})) - D(\mathbf{k})^2}. \quad (3)$$

Performing the Fourier transform, $\hat{G}^0(\mathbf{r}_i, \mathbf{r}_j, i\omega_n) = \sum_{\mathbf{k}\mathbf{k}'} \hat{G}^0(\mathbf{k}, \mathbf{k}', i\omega_n) e^{i\mathbf{k}\cdot\mathbf{r}_i - i\mathbf{k}'\cdot\mathbf{r}_j}$, of the Greens function with reference to the entries of Eqn. (3) gives

$$\hat{G}^0(\mathbf{r}_i, \mathbf{r}_j, i\omega_n) = \sum_{\mathbf{k}} [G_{11}^0(\mathbf{k}, i\omega_n) + G_{12}^0(\mathbf{k}, i\omega_n) e^{-i\mathbf{Q}\cdot\mathbf{r}_j} + G_{21}^0(\mathbf{k}, i\omega_n) e^{i\mathbf{Q}\cdot\mathbf{r}_i} + G_{22}^0(\mathbf{k}, i\omega_n) e^{i\mathbf{Q}\cdot(\mathbf{r}_i - \mathbf{r}_j)}] e^{i\mathbf{k}\cdot(\mathbf{r}_i - \mathbf{r}_j)}, \quad (4)$$

with the sum extending over the reduced Brillouin zone. The presence of scalar impurities is modelled by the following delta-function potentials

$$\hat{H}^{int} = \sum_{\{i\}\sigma} U_i \hat{n}_{i\sigma}, \quad (5)$$

where $\hat{n}_{i\sigma}$ is the density operator on site i . Here $\{i\}$ denotes the set of lattice sites hosting the impurities and U_i is the strength of the corresponding effective potential. In this article all the presented results arise from impurities modelled by a potential, $U = -15t$, corresponding to $-4.5eV$. In the DSC state this U generates resonances at a few meV for a single nonmagnetic impurity^{1,2,11}. The large scale of this potential renders the effects on the LDOS from corrections to other energy scales around the impurity site less important. For instance, we have checked that gap suppression near the impurity or slightly larger spatial extension of the impurity does not qualitatively affect the results reported below. In general these effects tend to push the resonances slightly further towards zero bias. We have also performed calculations (not shown here) with other values of U and comment on the results below.

The full Greens function $\hat{G}(\mathbf{r}, \omega)$ in the presence of the impurities can be obtained by solving the real-space Gorkov-Dyson equation

$$\hat{G}(\omega) = \hat{G}^0(\omega) \left(\hat{I} - \hat{H}^{int} \hat{G}^0(\omega) \right)^{-1}. \quad (6)$$

The size of the matrices in this equation depends on the number of impurities and the dimension of the Nambu space. We have previously utilized this method to study the electronic structure around impurities¹⁷ and vortices that operate as pinning centers of surrounding stripes²⁷. This method is identical to the traditional T-matrix formalism. However, for a numerical study of several impurities at arbitrary positions we find it easier to solve Eqn.

6 directly.

The 2D Fourier transform of the clean Greens function $\hat{G}^0(\mathbf{k}, \omega)$ is performed numerically by dividing the first Brillouin zone into a 800×800 lattice and introducing a quasi-particle energy broadening of $\delta = 1\text{meV}$ with δ defined from the analytic continuation $i\omega_n \rightarrow \omega + i\delta$. The differential tunnelling conductance is proportional to the LDOS which is determined from the imaginary part of the full Greens function.

So far nothing has been said about the form the band-structure. It is still controversial which quasi-particle energy applies to the DSC and DDW states^{22,25,26}. The expression for $\xi(\mathbf{k})$ is important since it will influence the final LDOS around the impurities. We illustrate this in the following by studying two generic band structures: the nested situation, and a t - t' band believed to be relevant for BSCCO around 10% hole doping. With the notation $\xi(\mathbf{k}) = \epsilon(\mathbf{k}) - \mu$, and

$$\epsilon(\mathbf{k}) = -2t(\cos(k_x) + \cos(k_y)) - 4t' \cos(k_x) \cos(k_y), \quad (7)$$

t (t') refers to the nearest (next-nearest) neighbor hopping integral and μ is the chemical potential. The nested situation corresponds to $t' = \mu = 0.0$ while the parameters for the 10% hole doped band are: $t = 300\text{meV}$, $t' = -0.3t$ and $\mu = -0.9t$. These parameters correspond to the ones previously studied for a single impurity by Morr²². As discussed in Ref. 22 there are physical reasons to expect the nested band to be relevant for the DDW state and the t - t' band for the DSC phase. However, recent photoemission measurements on LSCO by Zhou *et al.*²⁶ observed a Fermi surface consisting of straight lines connecting the antinodal regions which may indicate that the nested band is more relevant for impurity studies in LSCO. Thus we find it important for study both cases below.

In the results presented we include the LDOS filter¹¹. This effect modifies the LDOS, $\rho(\mathbf{r}, \omega) = \sum_n |\psi_n(\mathbf{r})|^2 \delta(\omega - \epsilon_n)$, by including the four nearest Cu neighbors in the underlying CuO_2 layer, $\psi_n(\mathbf{r}) \rightarrow \psi_n(\mathbf{r} + \mathbf{e}_x) + \psi_n(\mathbf{r} - \mathbf{e}_x) - \psi_n(\mathbf{r} + \mathbf{e}_y) - \psi_n(\mathbf{r} - \mathbf{e}_y)$. Here \mathbf{e}_i denote the unit vectors in the CuO_2 plane. It is important to keep in mind that the filtering effect is still controversial. However, determining experimentally the interference effects around two impurities in the DSC state may help resolve the relevance of the filter.

III. RESULTS

A. single impurity

Before studying the two impurity interference effects it is worthwhile to briefly review the single impurity LDOS in the DSC and DDW states and discuss the influence of the filter. Without the tunneling filter we find full agreement with previously published results^{7,15,20-22}. We will

see that a single impurity is not a good probe for distinguishing between these two states.

In the DDW phase one can utilize Eqn. (4) and (6) to calculate the full Greens function $\hat{G}(\mathbf{r}_i, \mathbf{r}_j, i\omega_n) = \hat{G}^0(\mathbf{r}_i - \mathbf{r}_j, i\omega_n) + \hat{G}^0(\mathbf{r}_i, i\omega_n)T(i\omega_n)\hat{G}^0(-\mathbf{r}_j, i\omega_n)$ with the T-matrix given by, $T(i\omega_n) = U[1 - UG^0(0, i\omega_n)]^{-1}$. The single resonance condition, $1 = U\text{Re}[G^0(0, \omega)]$, has been previously studied for the DDW state without the filtering effect^{20–22}. It is well known that the resulting LDOS strongly depends on the band structure. In Fig. 1a we plot the DOS in the clean DDW state for the nested and the t - t' band without the filter. Even though the above resonance condition is satisfied at certain energies for the t - t' band, we expect the large value of the DOS at all frequencies to overdamp the impurity peaks. This is contrary to the nested situation where a sharp impurity resonance is allowed to appear in the gap. This is clearly verified in Fig. 1b(c) which depicts the LDOS for the nested(t - t') set of band parameters including the filter. The peaks in Fig. 1c are not impurity resonances (note scale), which are overdamped, but simply the shifted DDW gap edges. The impurity can only slightly modify the amplitude of these gap edges. We note that it is t' which causes the impurity resonances to be strongly overdamped. When $t' = 0$, $\mu \neq 0$ the density of states always vanishes at minus the chemical potential²¹ allowing a well-defined resonance peak to appear.

As is evident from Fig. 1b the most important influence of the filter is to shift the LDOS maximum from the nearest neighbors to the impurity site and induce a second maximum on the next-nearest neighbor sites²⁸. This weight redistribution is identical to the situation in the superconducting phase¹¹.

In the DSC state, the clean DOS is plotted in Fig. 2a for both the nested and the t - t' band. By comparison to Fig. 1a we see the well known result that the nested DOS is identical for the clean DDW and DSC phase. Indeed this motivated the original studies of single impurity resonances in the DSC versus DDW states^{20–22}. The single impurity resonance condition in the DSC phase, $1 = U\text{Re}[G^0(0, \pm\omega)]$, generates peaks at positive and negative energies around a single nonmagnetic impurity. However, the majority of the quasi-particle weight may reside on only one of these resonances¹⁷.

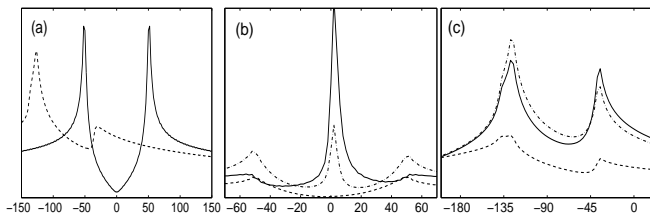


FIG. 1. DOS (arb. units) as a function of energy (meV) in the DDW state: (a) for the clean system with nested (solid) or t - t' (dashed) band. (b) DOS at (0,0) (solid), (1,0) (dashed), and (1,1) (dash-dotted) for a nested band with the impurity at (0,0). (c) same as (b) but for a t - t' band.

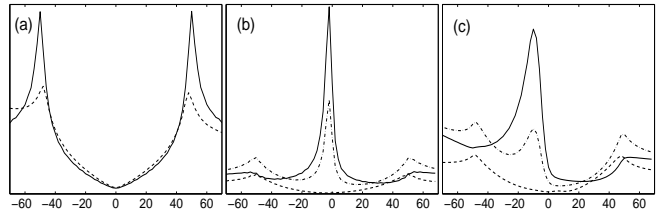


FIG. 2. Same as Fig. 1 but for the DSC state.

It is evident from *both* Fig. 2b and Fig. 2c that indeed only one resonance has weight. This is contrary to the situation without the filter²². Thus by comparing Fig. 1b to Fig. 2b (or 2c) the result is two almost identical figures. Therefore, since no qualitative difference is guaranteed to exist the single nonmagnetic impurity cannot easily distinguish the DSC and DDW phases. However, as shown below, the interference between several impurities can be utilized to *tune the amplitude* of the potential resonances and thus clearly distinguish the phases.

The impurity LDOS plotted in Fig. 1 and Fig. 2 was for $U = -15t$. Though of less experimental relevance, we briefly mention another difference between the DSC and DDW states. This relates to the fate of the resonance in the unitary limit, $U \rightarrow \infty$: for the DDW phase the resonance energy approaches minus the chemical potential, $\omega = -\mu$, whereas it approaches the Fermi level in the DSC phase (except for a small residual energy shift caused by a possible particle-hole asymmetry²⁹). The different resonance energy (as $U \rightarrow \infty$) arises from the way the chemical potential enters the bands of the clean DDW ($E_{\pm}(\mathbf{k}) = |\sqrt{\epsilon(\mathbf{k})^2 + D(\mathbf{k})^2} \pm \mu|$) and DSC ($E_{\pm}(\mathbf{k}) = \sqrt{(|\epsilon(\mathbf{k})| \pm \mu)^2 + \Delta(\mathbf{k})^2}$) states^{20,21}.

B. two impurities, nested band

In general when several impurities are in close proximity the resonances split, and one expects to see additional peaks in the density of states. The evolution of the LDOS as a function of distance and angular orientation between two nonmagnetic impurities in the DSC state has been already studied by several authors^{15–17}. In the following we elaborate on this work by a numerical study of the LDOS including the filtering effect and study for the first time the quantum interference between two strong nonmagnetic impurities in the DDW state. In the superconducting phase Fig. 3a shows the resulting LDOS for the nested band when one impurity is fixed at the origin (0,0) while the other is moved out along a crystal axis to (10,0). In Fig. 3b the impurities are fixed at (−1,0) and (+1,0) while the STM tip is moved from (0,0) to (8,0). As seen from both figures there are strong variations in the LDOS in agreement with previous studies without the extra tunnelling effect^{15,17}.

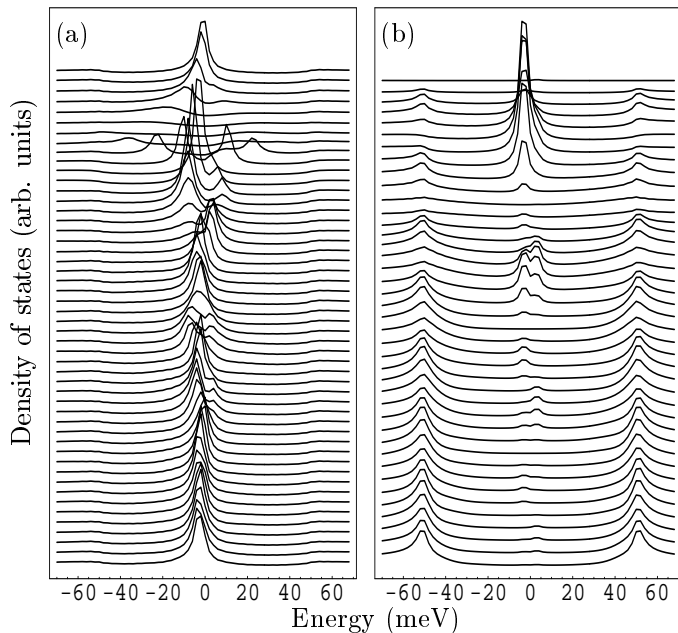


FIG. 3. (a) DOS at $(0,0)$ as a function of the distance between two nonmagnetic impurities (here: $t' = \mu = 0.0$). One impurity is fixed at $(0,0)$ while the other moves from $(0,0)$ (top) to $(10,0)$ (bottom). (b) the impurities are fixed at $(\pm 1,0)$ while the STM tip is moved from $(0,0)$ (top) to $(8,0)$ (bottom). The difference between each scan is 0.2 lattice constants and the graphs are off-set for clarity.

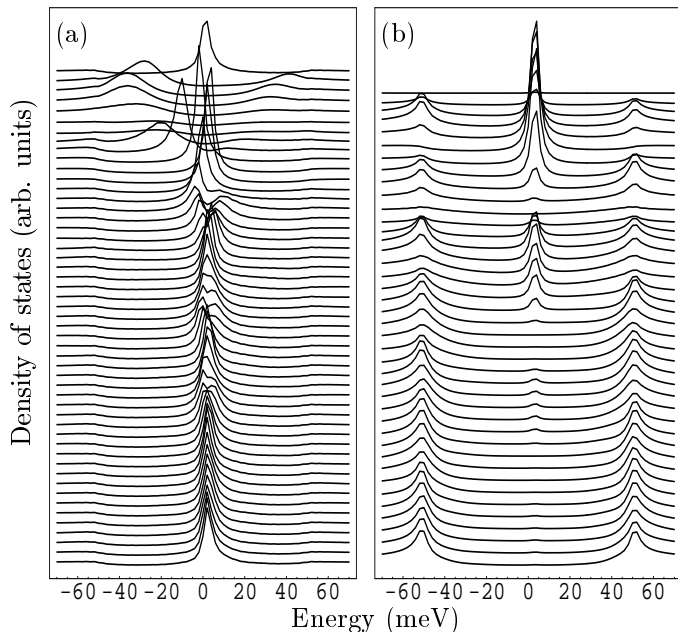


FIG. 4. Same as Fig. 3 but for the d-density wave state.

The number of apparent resonances, their energetic position and width strongly depend on the impurity configura-

tion and the position of the STM tip. In particular, for certain impurity separations the resonances completely disappear. In Fig. 4 we show the LDOS for the same impurity and STM positions as in Fig. 3 but for the DDW state. Clearly, strong quantum interference between the two nonmagnetic impurities also exists in this state. However, by comparison with Fig 3 it is evident that the additional resonance states in the DSC allows one to distinguish this from the DDW phase. We have performed identical calculations to the ones presented in Fig. 3-4 for other (but still large) values of the scattering potential U , and always find qualitatively the same interference pattern.

As mentioned above, the resonances split when two impurities are in close proximity. It is therefore nontrivial that only a single, nondispersive peak is seen in e.g. Fig. 4b. This is closely connected to the particular STM scan and one may worry about the robustness of this result. However, we always find that whenever the impurity positions are invariant under mirror reflection through the STM scan line, only a single nondispersive peak remains³⁰ in the DDW state. Importantly, for these same configurations we find the alternating double peak structure (similar to Fig. 3b,5b) to be a robust feature in the superconducting phase. Furthermore, as expected for a d-wave gap¹⁷, we find (not shown) that the quantum interference patterns are longer ranged along the nodal directions than along the Cu-O bonds.

As expected from the discussion of the single impurity in the DDW state, we end this section by noting that when $t' = 0.0$, $\mu \neq 0.0$ the interference pattern is identical to that shown in Fig. 4 except for a shifted (by $-\mu$) energy range.

C. two impurities, $t-t'$ band

We now turn to the quasi-particle dispersion given by Eqn. (7) with $t' = -0.3t$, $\mu = -0.9t$. In this case we know from Fig. 1a and Fig. 2a that the clean DOS is clearly different in the DDW and DSC states. This section serves as an illustration of the importance of the quasi-particle dispersion in the final LDOS. Fig. 5 shows the LDOS in the superconducting phase from the same STM and impurity positions as Fig. 3. It is clear that again the strong interference between the impurity wavefunctions survive the filtering effect and pose new constraints on the potential scattering scenario versus more strongly correlated models⁵. We note that despite the very different band structure used to calculate the LDOS in Fig. 3 and Fig. 5, the overall evolution of the resonances is quite similar except that the apparent resonances are shifted to higher energies for the $t-t'$ band. As mentioned above, it has been previously suggested that the nested ($t-t'$) band is appropriate for the DDW (DSC) state²². In that case we need compare Fig. 4 and Fig. 5. As opposed to the single impurity LDOS, the

configuration in Fig. 4b and Fig. 5b again allows one to distinguish the DDW and DSC states by the number of resonance peaks. This is contrary to Fig. 4a and Fig. 5a which are remarkably similar.

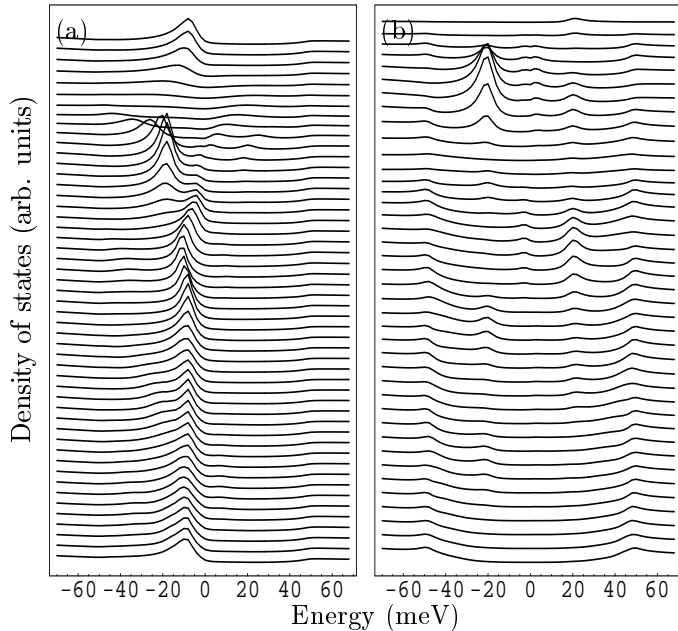


FIG. 5. Same as Fig. 3 but for $t' = -0.3t$ and $\mu = -0.9t$.

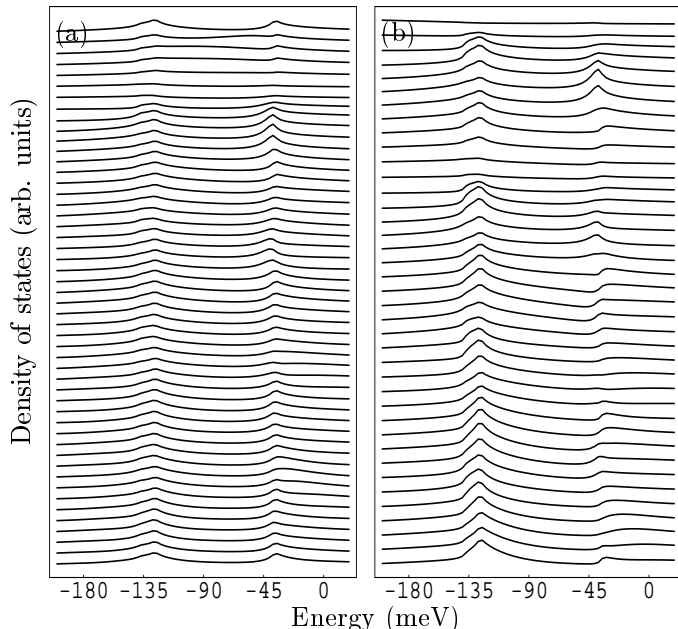


FIG. 6. Same as Fig. 5 but for the d-density wave state. Note the energy range. The peaks evident in these scans are the shifted DDW gap edges (not impurity resonances).

In the DDW phase we know from the single impurity case that the current choice of band parameters leads to strongly overdamped impurity resonances (Fig. 1c). However, for completeness we show the calculated STM scans in Fig. 6. As expected the quantum interference is weak and causes only minor changes in the DDW gap edges. Furthermore, the LDOS shown in Fig. 6 changes only slightly upon varying U or the impurity positions.

IV. CONCLUSION

In summary we have shown that a systematic STM study around two nonmagnetic impurities can clearly distinguish the DSC and DDW phases. In particular, we suggest to perform STM scans with the positions of the impurities being invariant under a mirror reflection through the scan line. Even for the nested band, where the clean and the single impurity LDOS are not a good probe for the underlying state, this situation provides a robust test for DSC versus DDW order.

The impurities are modelled as potential scatterers and the results pose further tests on this approach. An important question remains whether phase fluctuations present about T_c in the pseudo-gap state are strong enough to wash out the interference patterns. This will be discussed in a future publication³¹. It would also be interesting to study similar multiple impurity interference effects within other pseudo-gap models and within other proposed scenarios for the resonances around nonmagnetic impurities in d-wave superconductors. In particular, within models explaining the single impurity LDOS as a Kondo resonance arising from a confined spinon^{5,32}, one may expect more novel changes as the distance between two nonmagnetic impurities is decreased. This is because the cost of frustrated dimers decrease in this limit making it unfavorable to break another dimer, and hence no spin is expected near the nonmagnetic impurities.

I acknowledge stimulating correspondence with P. Hedegård, J. Paaske, S. Sachdev, and J.-X. Zhu. This work is supported by the Danish Technical Research Council via the Framework Programme on Superconductivity.

-
- ¹ A. Yazdani, C.M. Howald, C.P. Lutz, A. Kapitulnik, and D.M. Eigler, *Phys. Rev. Lett.* **83**, 176 (1999).
 - ² S.H. Pan, E.W. Hudson, K.M. Lang, H. Eisaki, S. Uchida, and J.C. Davis, *Nature* **403**, 746 (2000).
 - ³ L. Yu, *Acta Phys. Sin.* **21**, 75 (1965); H. Shiba, *Prog. Theo. Phys.* **40**, 435 (1968).
 - ⁴ A.V. Balatsky, M.I. Salkola, and A. Rosengren, *Phys. Rev.*

- B **51** 15547 (1995); M.I. Salkola, A.V. Balatsky, and D.J. Scalapino, Phys. Rev. Lett. **77**, 1841 (1996).
- ⁵ M. Vojta, Y. Zhang, and S. Sachdev, Phys. Rev. Lett. **85**, 4940 (2000); Phys. Rev. **62**, 6721 (2000); Z. Wang, and P.A. Lee, Phys. Rev. Lett. **89**, 217002 (2002); A. Polkovnikov, S. Sachdev, and M. Vojta, Phys. Rev. Lett. **86**, 296 (2001); K. Park, cond-mat/0203142; M. Vojta and R. Bulla, Phys. Rev. B **65**, 014511 (2001).
- ⁶ J.E. Hoffman, K. McElroy, D.-H. Lee, K.M. Lang, H. Eisaki, S. Uchida, and J.C. Davis, Science **297**, 1148 (2002); K. McElroy, R.W. Simmonds, J.E. Hoffman, D.-H. Lee, J. Orenstein, H. Eisaki, S. Uchida and J.C. Davis, Nature **422**, 592 (2003).
- ⁷ Q.-H. Wang and D.-H. Lee, Phys. Rev. B **67**, 020511 (2003).
- ⁸ D. Zhang, and C.S. Ting, Phys. Rev. B **67**, 100506 (2003).
- ⁹ L. Zhu, W.A. Atkinson, and P.J. Hirschfeld, cond-mat/0307228.
- ¹⁰ L. Capriotti, D.J. Scalapino, and R.D. Sedgewick, cond-mat/0302563.
- ¹¹ I. Martin, A.V. Balatsky, and J. Zaanen, Phys. Rev. Lett. **88**, 097003 (2002).
- ¹² See also: J.-X. Zhu, C.S. Ting and C.R. Hu, Phys. Rev. B **62**, 6027 (2000).
- ¹³ H. Alloul *et al.*, Phys. Rev. Lett. **67**, 3140 (1991); J. Bobroff *et al.*, Phys. Rev. Lett. **83**, 4381 (1999); A.V. Mahajan *et al.*, Europhys. Lett. **46**, 678 (2000); M.-H. Julien *et al.*, Phys. Rev. Lett. **84**, 3422 (2000).
- ¹⁴ H.C. Manoharan, C.P. Lutz, and D.M. Eigler, Nature **403**, 512 (2000).
- ¹⁵ D. Morr, and N.A. Stavropoulos, Phys. Rev. B **66**, 140508 (2002).
- ¹⁶ L. Zhu, W.A. Atkinson, and P.J. Hirschfeld, Phys. Rev. B **67**, 094508 (2003); W.A. Atkinson, P.J. Hirschfeld, and L. Zhu, cond-mat/0301630.
- ¹⁷ B.M. Andersen, and P. Hedegård, Phys. Rev. B **67**, 172505 (2003).
- ¹⁸ D.J. Derro *et al.*, Phys. Rev. Lett. **88**, 097002 (2002); D.K. Morr, and A.V. Balatsky, Phys. Rev. Lett. **90**, 067005 (2003).
- ¹⁹ S. Chakravarty, R.B. Laughlin, D.K. Morr, and C. Nayak, Phys. Rev. B **63**, 094503 (2001).
- ²⁰ J.-X. Zhu, W. Kim, C.S. Ting, and J.P. Carbotte, Phys. Rev. Lett. **87**, 197001 (2001).
- ²¹ Q.-H. Wang, Phys. Rev. Lett. **88**, 057002 (2002).
- ²² D. Morr, Phys. Rev. Lett. **89**, 106401 (2002).
- ²³ H.K. Nguyen, and S. Chakravarty, Phys. Rev. B **65**, 180519 (2002); S. Chakravarty, H.-Y. Kee, and C. Nayak, Int. J. Mod. Phys. B **15**, 2901 (2001); X. Yang, and C. Nayak, Phys. Rev. B **65**, 064523 (2002).
- ²⁴ T. Pereg-Barnea and M. Franz, cond-mat/0306712.
- ²⁵ M. Norman, Phys. Rev. B **63**, 092509 (2001).
- ²⁶ X.J. Zhou *et al.*, Phys. Rev. Lett. **86**, 5578 (2001).
- ²⁷ B.M. Andersen, P. Hedegård, and H. Bruus, Phys. Rev. B, **67**, 134528 (2003); J. Low. Temp. Phys. **131**, 281 (2003).
- ²⁸ Compare for instance to Fig. 1 in Ref. 20.
- ²⁹ R. Joynt, J. Low. Temp. Phys. **109**, 811 (1997).
- ³⁰ This is also valid when the impurity positions coincide with the STM scan line as in Fig. 3b-6b.
- ³¹ B.M. Andersen, unpublished.
- ³² See also: S. Sachdev, Rev. Mod. Phys. **75**, 913 (2003).